Safety and Lateral Dynamics Improvement of a Race Car Using Active Rear Wing Control

Conference Paper · April 2019

DOI: 10.4271/2019-01-0643

3 authors:

Mohammed Hammad
Ontario Tech University
3 PUBLICATIONS **5** CITATIONS
SEE PROFILE

Khizar Qureshi
Ontario Tech University
2 PUBLICATIONS **7** CITATIONS
SEE PROFILE

Yuping He
Ontario Tech University
157 PUBLICATIONS **1,266** CITATIONS
SEE PROFILE

2019-01-0643 Published 02 Apr 2019

Safety and Lateral Dynamics Improvement of a Race Car Using Active Rear Wing Control

Mohammed Hammad, Khizar Qureshi, and Yuping He University of Ontario Institute of Technology

Citation: Hammad, M., Qureshi, K., and He, Y., "Safety and Lateral Dynamics Improvement of a Race Car Using Active Rear Wing Control," SAE Technical Paper 2019-01-0643, 2019, doi:10.4271/2019-01-0643.

Abstract

As the forward speed of a car increases, the safety of the vehicle and the driver becomes a more significant concern. Active aerodynamic control can effectively enhance the lateral stability of high speed vehicles over tight cornering maneuvers. A split rear wing has been proposed. By means of manipulating the attack angles for the right and/or left parts of the split rear wing, a favorable yaw moment may be achieved to ensure the lateral stability of the vehicle. However, active control of the split rear wing has not been adequately explored. This paper proposes a novel active split rear wing, which can improve the lateral stability over tight cornering maneuvers, and will not degrade the longitudinal dynamics of the vehicle. A Linear Quadratic Regulator (LQR) based controller for the active split rear wing is designed using a linear vehicle model. In order to examine the performance of the active split rear wing, Numerical simulation is carried out using the LQR based controller and a yaw-plane vehicle model designed in MATLAB. The effectiveness of the proposed active split rear wing is demonstrated by the results derived from the numerical simulation.

Introduction

Improving road infrastructure has led to increasing the average forward speeds of a car. Consequently, the risk of losing stability and control has increased. This is the case under tight cornering maneuvers of high-speed vehicles. Motorsports assume higher speeds and challenging curves for the driver to negotiate. Consequently, the forward speed of a race car is also increasing by every passing year on any track [1], and with increasing speeds, safety deserves more attention. While various measures have been taken to increase the speed and the safety of a vehicle, e.g., drag reduction, tire design improvement, improving the robustness of the cockpit/cabin and deployment of airbags, etc., this paper examines a control strategy to utilize the aerodynamic forces to improve both the lateral dynamics and safety. This may be achieved by employing a split rear wing to generate a favorable yaw moment and downward forces. It should be mentioned that active aerodynamic control devices have not been applied to most of the racing competitions due to various reasons, including the reliability concerns of these advanced active safety systems. This paper intends to address the potential capabilities of the active aerodynamic control device for improving the lateral stability of high-speed vehicles. The results of this research form a basis to develop control schemes and evaluate the effectiveness of improving the lateral stability and safety with more accurate vehicle and wing models. It is expected that the research results derived from this research will contribute to the ultimate application of the advanced active safety technique to motorsports.

Conventional rear wings (with a fixed posture) installed on a car introduce drag and produce downforce. These wings lack the ability of adjusting the attack angles to adaptively manipulate the drag and lift/downforce according to operating conditions. In contrast, active rear wings can adaptively adjust the attack angles to effectively reduce aerodynamic drag and produce required lift/downforce in order to improve the acceleration performance and enhance the lateral stability of the vehicle. Aerodynamic drag degrades the longitudinal acceleration performance of a road vehicle. A downforce may impose multifold impacts on the dynamics of the vehicle. A downforce instead of a lift may increase the yaw- and roll-stability of the vehicle; the downforce may also lead to the increase of tractive force due to increased normal force of driving wheels [2]; furthermore, if the wing is split, it can be used to generate favorable yaw and roll moments by manipulating the attack angles of the left and right sections of the wing and the vehicle's safety can be increased [3, 4]. Understandably, the posture of the wing(s) in terms of attack angles should adaptively vary under varied operating conditions. A vehicle travelling in a straight line will not need additional drag forces; a smaller turn radius will need a higher yaw moment than the turn with larger radius; tight cornering also requires drag force to the effect of braking. Therefore, a strategy to control the attack angles according to varied operating conditions is proposed in this paper.

The rest of the paper is organized as follows. In Section 2, the modelling of the vehicle system, including tire and wing dynamics, will be introduced, and the vehicle system

model will be validated. Section 3 designs the control scheme for the split wing. Section 4 presents and discusses the simulation results. Finally, the conclusions will be drawn in Section 5.

Vehicle System Modelling

To design a dynamic control system, conducting mathematical modelling is the first and necessary step towards designing its control system. A road vehicle is a complex system consisting of numerous subsystems and components. In vehicle system modelling and simulation, there is a trade-off between the complexity of the vehicle model and the computational efficiency. To achieve a compromised solution regarding the trade-off, in the vehicle system modelling of this research, the following assumptions have been made:

- The steering angles for the two front tires are equal.
- The steering angles of the front tires are small.
- The vehicle forward speed is constant.
- The pitch, roll and vertical motions are not considered.
- The vehicle system is represented by a bicycle model.

Based on the aforementioned assumptions, a simplified vehicle model with a split rear wing is shown in Figure 1.

FIGURE 1 (a) Forces acted on the vehicle system through tires and wings, (b) vertical forces applied on the vehicle system, (c) kinematic analysis of the vehicle system.

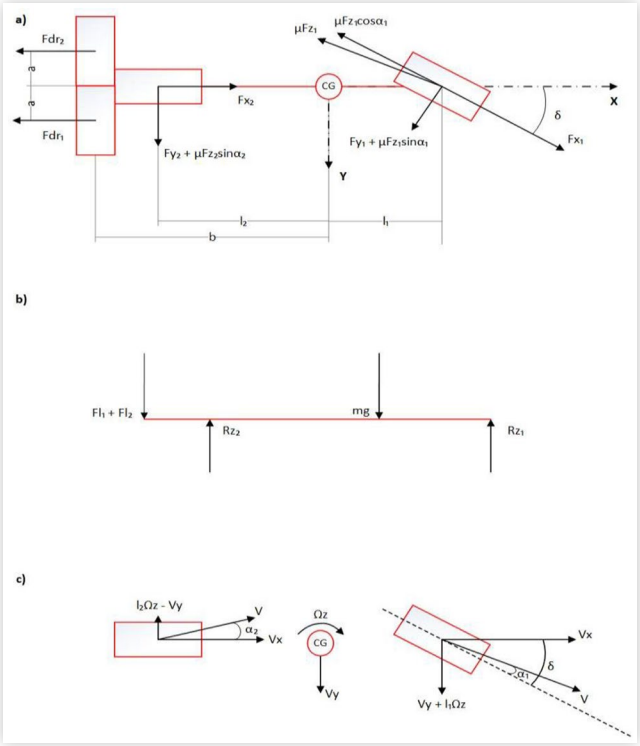

In the vehicle system modelling, the SAE Coordinate System is used [5]. The governing equations of motion for the vehicle system can be expressed as

$$m\left(\dot{V}_y + V_x\Omega_z\right) = \left(F_{y1} + \mu F_{z1}\alpha_1\right) + \left(F_{y2} + \mu F_{z2}\alpha_2\right) \quad (1)$$

$$I_{zz}\dot{\Omega}_z = l_1\left(F_{y1} + \mu F_{z1}\alpha_1\right) - l_2\left(F_{y2} + \mu F_{z2}\alpha_2\right) + a\left(F_{dr1} - F_{dr2}\right) \quad (2)$$

where the notation of the parameters is provided in Appendix 1 and is shown in Figure 1. Note that the vehicle model represented by Equations (1) and (2) is different from the conventional bicycle model in that the aerodynamic drags, in terms of F_{dr1} and F_{dr2}, and downforces, in terms of F_{z1} and F_{z2}, are considered. Equations (1) and (2) can be rewritten in the state-space form as

$$\dot{x} = Ax + Bu \quad (3)$$

$$y = Cx + Du \quad (4)$$

where the state variable vector is defined as

$$\dot{x} = \left[V_y\ \Omega_z\ y\ \Psi\right]^T \quad (5)$$

and the input vector is specified as

$$u = \left[\delta\ \theta_1\ \theta_2\right]^T \quad (6)$$

where θ_1 and θ_2 denote the angle of attack of the right and left section of the split wing. The following subsections introduce the modelling of tire and wing.

Tire Model

The front and rear tire cornering forces can be expressed as a function of the tire's cornering stiffness and the slip angle [6],

$$F_{y1} = C_f\alpha_1; F_{y2} = C_r\alpha_2 \quad (7)$$

where slip angles of the front and rear tires are determined as

$$\alpha_1 = \delta - \frac{\left(V_y + a\Omega_z\right)}{V_x} \quad (8)$$

and

$$\alpha_2 = \frac{-V_y + b\Omega_z}{V_x} \quad (9)$$

Downforce Distribution

The downward force on each tire is determined by performing dynamic analysis as shown in Figure 1(b). The two downward forces from the two separate wings acting through the center line of the vehicle are expressed as

$$R_{z1} = m\left(\frac{l_2}{l_1 + l_2}\right) - F_l\left(\frac{b - l_2}{l_1 + l_2}\right) \quad (10)$$

$$R_{z2} = m\left(\frac{l_1}{l_1 + l_2}\right) + F_l\left(\frac{b + l_1}{l_1 + l_2}\right) \quad (11)$$

where,

$$F_l = F_{l1} + F_{l2} \quad (12)$$

Wing Model

The drag and lift forces on any object can be expressed as a function of the drag and lift coefficients, density of the fluid, relative velocity and the projected area of the object [2, 16] and are given as,

$$F_{Drag} = \frac{C_D \rho v_x^2 A}{2} \tag{13}$$

$$F_{Lift} = \frac{C_L \rho v_x^2 A}{2} \tag{14}$$

The wing forces can be modelled similarly with the only change occurring in the projected area of the wing, which changes with changing attack angle as shown in Figure 2. This model is validated by a similar model proposed in an earlier work [7]. Keeping the small angle approximation in affect the equations can be written as,

$$F_{dri} = \frac{C_D \rho v_x^2 A_w \theta_i}{2} \tag{15}$$

$$F_{li} = \frac{C_L \rho v_x^2 A_w \theta_i}{2} \tag{16}$$

where i= 1 and 2, meaning the left and right sections of the rear split wing, respectively. Note that as shown in Figure 1(a), geometrically the right and left sections of the rear split wing are design symmetric.

The rear split wing is designed to operate in two modes, namely integral and split. In the integral mode, the right and left sections of the rear split wing are combined into an integral unit, and the aerodynamic drag and downforce of the unit can be manipulated by varying the attack angle. Using the integral mode, the pitch moment of the vehicle sprung mass can be controlled to improve the dynamic performance of the vehicle, e.g., improving the ride quality during panic braking or heavy acceleration process. In the split mode, the right and left sections of the rear split wing can operate independently by separately adjusting the attack angle of the individual sections. Operating in the split mode, the right and left downforces can be controlled and coordinated so that the roll moment of the sprung mass can be manipulated in order to enhance the roll stability of the vehicle. Moreover, if the split mode is jointly designed with the electronic stability control (i.e., differential braking) system, the yaw moment control functionality may be significantly enhanced.

FIGURE 2 Description of the attack angle of the wing.

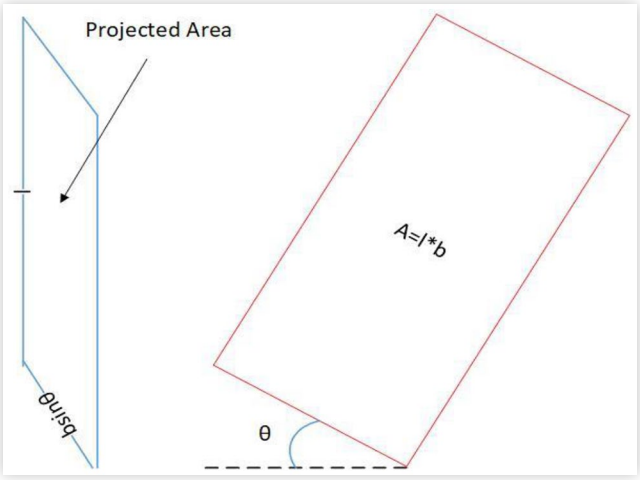

TABLE 1 Vehicle system parameters.

Symbol	Description	Value
m	Mass of the vehicle	1700 kg
l_1	Distance of CG from front axle	1.5 m
l_2	Distance of CG from rear axle	1.7 m
a	Perpendicular distance of the point of application of drag force from the vehicle centerline	0.8 m
b	Distance of the wing from the CG of vehicle	1.7 m
A_w	Planform area [8] of the wing at zero attack angle	0.24 m^2
ρ	Density of air	1.225 kg/m^3
μ	Coefficient of friction of tire-road surface	0.7
C_f	Cornering stiffness of front tires	40000 N/rad
C_r	Cornering stiffness of rear tires	40000 N/rad
C_L	Lift coefficient of each wing	1.25
C_D	Drag coefficient of each wing	1
I_{zz}	Mass moment of inertia of the vehicle	2000 kg. m^2

Vehicle Parameters

The drag and lift coefficient values depend on the type of wing selected. Previous studies have demonstrated the effectiveness of the Seig S1223 airfoil design for the rear split wing [3, 4, 15]. The values of the coefficients in Equations (15) and (16) are selected based on these studies. Table 1 offers the other vehicle system parameters, which are determined using the numerical simulation based on EOM software package [17]. Note that EOM is a multibody dynamic software, which can automatically generate the governing equations of motion of the selected vehicle model.

Vehicle System Model Validation

The vehicle system model represented by Equations (3) to (6) has been validated using EOM Software, which can generate linearized equations of motion of any given mechanical system upon description of the system geometry.

With an input file describing the specified geometry configuration of the vehicle with the required system parameters listed in Table 1, EOM software automatically generations the governing equations of motion of the vehicle system in state-space format. The resulting matrices ***A,B,C*** and ***D*** based on EOM software are identical to those derived from the research.

Active Aerodynamic Control System Design

This section briefly introduces the active aerodynamic controller for controlling the attack angles of the rear split wing. The controller is designed using the Linear Quadratic Regulator (LQR) technique. Then, the active aerodynamic control scheme is presented.

LQR-Based Controller

The LQR technique is frequently used to design feedback controllers to provide optimal control of dynamic systems to ensure operation at minimum cost [9, 10]. The continuous-time linear vehicle system in infinite-horizon is represented in Equation (3). The LQR cost function is defined as,

$$J = \int_0^\infty \left(\boldsymbol{x}^T \boldsymbol{Q} \boldsymbol{x} + \boldsymbol{u}^T \boldsymbol{R} \boldsymbol{u} \right) dt \tag{17}$$

where Q and R represent the weighting matrices that penalize the magnitude and duration of the states and control inputs respectively. The desired performance of the system is defined by the Q and R matrices.

Control Scheme

Improving the lateral stability and increasing the safety of the high-speed vehicle is the goal of the control system. To ensure good handling performance and high lateral stability of road vehicles, the yaw rate and lateral acceleration based on a reference model are commonly selected as the desired control variables for electronic stability control system design [11]. Inspired by this concept, a reference model tracking control method is proposed for the active aerodynamic control scheme. The mathematical expressions for the reference yaw rate and lateral acceleration, respectively, are as follows,

$$\Omega_{z,ref} = \frac{V}{L + K_{us} V^2 / g} \delta \tag{18}$$

$$a_{y,ref} = \frac{V^2}{gL + K_{us} V^2} \delta \tag{19}$$

where the understeer coefficient K_{us} is given by,

$$K_{us} = \frac{mgl_2}{2lC_f} - \frac{mgl_1}{2lC_r} \tag{20}$$

The LQR-based controller is designed to track the reference values and reduce the error between the actual and reference values. The error values are fed into the LQR-based controller to compute the optimal values of the attack angles. The two attack angles of the two sections of the rear split wing are the input to the virtual vehicle represented by Equations (3) to (6). With the given input, the angular actuators will manipulate the attack angles of the right and left sections of the rear split wing to produce the required downforces to stabilize the car at high speeds under cornering maneuvers.

In the control system design, the input of the two attack angles is set to be zero initially. The feedback from the outputs, then, is used to vary the attack angles automatically. As the attack angles change, favorable forces and moments are applied to the vehicle system according the equations presented in earlier sections and stabilize the vehicle.

Simulation Results and Discussion

In order to evaluate the effectiveness of the proposed active aerodynamic control system, a benchmark investigation is conducted by comparing the numerical simulation results based on the designs with and without the active safety control. For the purpose of comprehensively assessing the directional performance of the designs at varied speeds, an obstacle avoidance maneuver at the forward speeds of 100, 150 and 200 km/h is simulated. To implement the obstacle avoidance maneuver, we adopt the front wheel steer input in terms of a single sine wave with an amplitude of 0.03 radians and a time period of 3 seconds, which is shown in Figure 3. Note that the specified steer input will execute a single lane change (SLC) maneuver [12]. Note that the design without the active safety control corresponds to the vehicle equipped with a fixed rear wing without the function of adjusting the attack angles.

Figures 4 and 5 compare the simulation results of the designs with and without the active aerodynamic control in terms of the time history of the yaw rate and the lateral acceleration, respectively. As shown in Figures 4 and 5, the dynamic responses for the two designs are almost identical. This implies that the active control system show no effect at the speed of 100 km/h.

Figures 6 and 7 display the yaw rate and the lateral acceleration at the speed of 150 km/h, respectively. It is found that the active aerodynamic control slightly suppresses both the yaw rate and the lateral acceleration. Results shown in

FIGURE 3 A sine wave representing a single lane change maneuver.

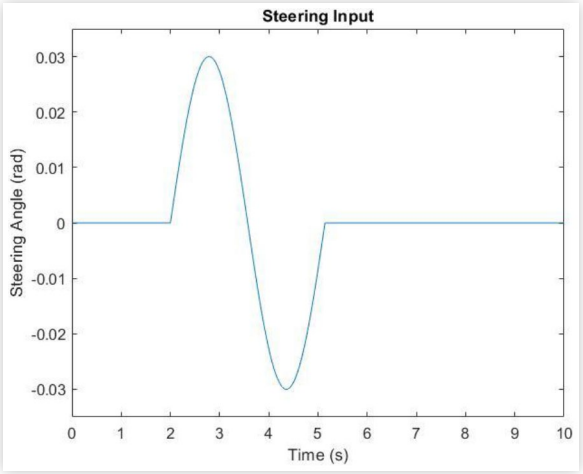

FIGURE 4 Yaw rate of the vehicle at 100 km/h.

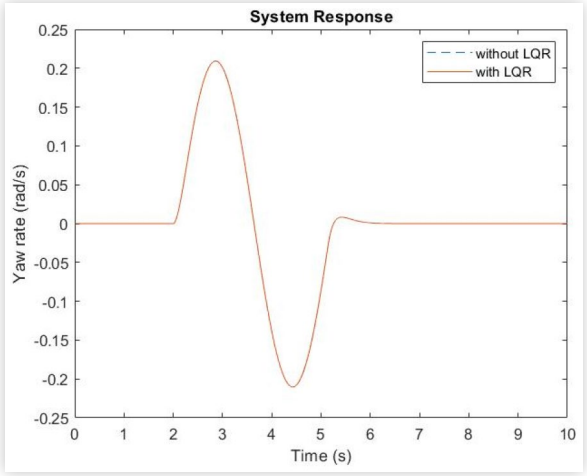

FIGURE 5 Lateral acceleration at the CG of the vehicle at 100 km/h.

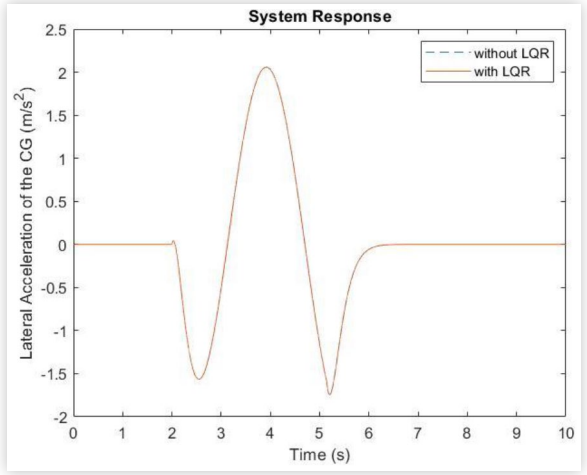

Figures 6 and 7 indicate that under the condition of implementing the SLC maneuver, the control system can improve the yaw and roll stability of the vehicle with smaller yaw rate and lateral acceleration. However, the extent of the lateral stability improvement due to the active control system is not appreciable at the speed of 150 km/h.

Figures 8 and 9 show the yaw rate and the lateral acceleration at the speed of 200 km/h, accordingly. Compared with the design without the active aerodynamic control, the LQR controller significantly suppress both the yaw rate and the lateral acceleration. Thus, at the forward speed of 200 km/h, the active aerodynamic control system can appreciably improve both the yaw and roll stability of the vehicle under the evasive maneuver. It is expected that the control system can further improve the lateral stability of the vehicle as the forward speed increases.

The simulation results shown in Figures 4 to 9 reveal that the active aerodynamic control system is not effective at speed lower than 100 m/h, and it exhibits its effectiveness at speed higher than 150 km/h. In other words, the higher the forward speed the vehicle travels, the more effectively the active

FIGURE 6 Yaw rate of the vehicle at 150 km/h.

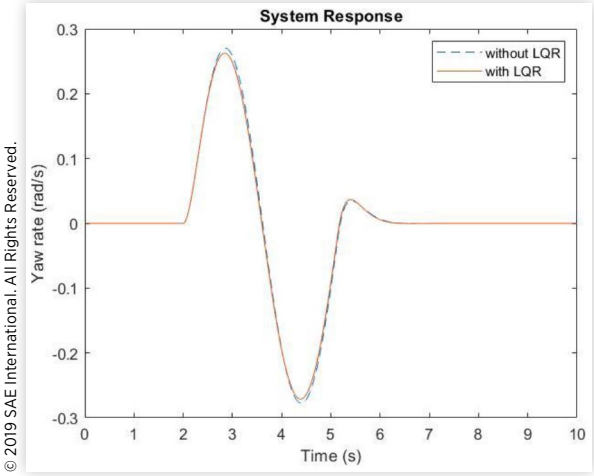

FIGURE 7 Lateral acceleration of the CG of the vehicle at 150 km/h.

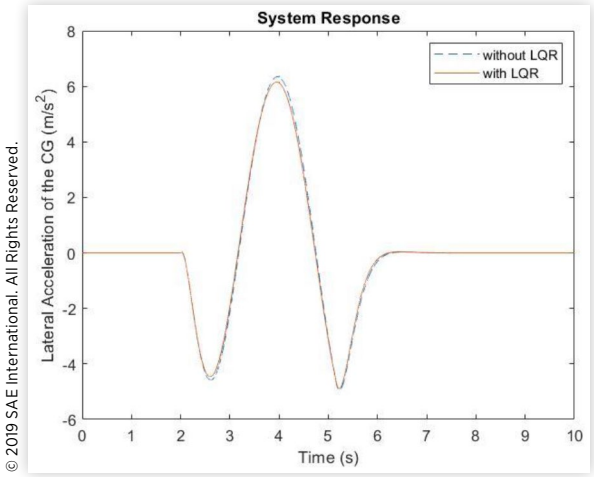

FIGURE 8 Yaw rate of the vehicle at 200 km/h.

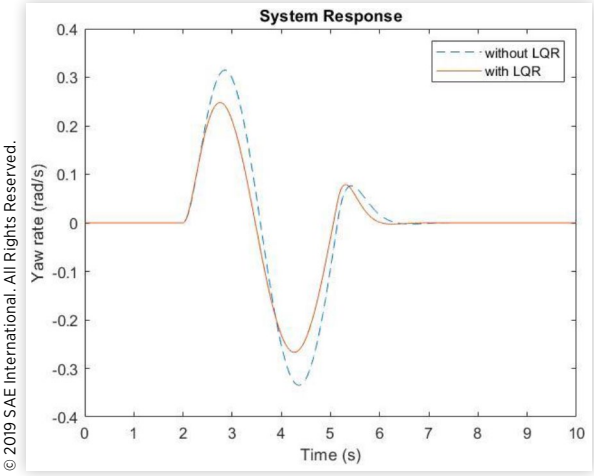

FIGURE 9 Lateral acceleration of the CG of the vehicle at 200 km/h.

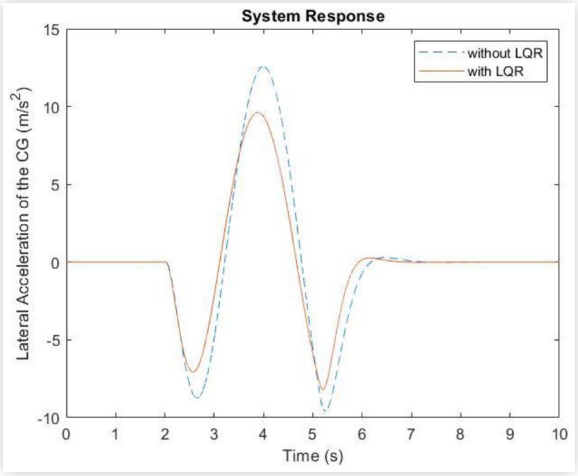

aerodynamic control system operates. This dynamic phenomenon of the active aerodynamic control system may be attributed to the relationship between the downforce and vehicle forward speed v_x expressed in Equation (16) and the relationship between the drag and vehicle forward speed v_x described in Equation (15).

Conclusions

This paper presents an active aerodynamic control system for improving the lateral stability of road vehicles under high-speed cornering maneuvers. To implement the conceptual design, a linear vehicle model with the function of a rear split wing is developed. The active aerodynamic control is realized by adaptively adjusting the attack angles of the right and left sections of the rear split wing. By means of the active aerodynamic control, the drags and downforces produced by the right and left sections of the rear split wing can be controlled and coordinated in order to improve the lateral stability of high-speed vehicle under tight cornering maneuvers. The controller for the active aerodynamic control system is designed using the LQR technique. Numerical simulation demonstrates the effectiveness of the active aerodynamic control system under high-speed evasive maneuver.

In the near future, the active aerodynamic control system will be further improved and validated using realistic vehicle models, e.g., CarSim software, and wind tunnel testing. Moreover, the effect of the front split wing control on the lateral stability of high-speed vehicle will be explored.

References

1. https://www.formula1.com/en/results.html/2017/races/975/united-states/fastest-laps.html
2. Barnard, R.H., *Road Vehicle Aerodynamic Design: An Introduction* (MechAero Pub, 2009). ISBN:9780954073473.
3. Sikder T., Kapoor S., He Y., "Optimizing Dynamic Performance of High-Speed Road Vehicles Using Aerodynamic Aids," in *ASME International Mechanical Engineering Congress and Exposition, Volume 7: Fluids Engineering*, V007T09A060, doi:10.1115/IMECE2016-65414.
4. Ayyagari, D.T. and He, Y., "Aerodynamic Analysis of an Active Rear Split Spoiler for Improving Lateral Stability of High-Speed Vehicles," *International Journal of Vehicle Systems Modelling and Testing* 12(3/4):100-100, 2017, doi:10.1504/IJVSMT.2017.10011079.
5. SAE International, "Vehicle Dynamics Terminology," SAE Standard J670_200801, Rev. Jan. 2008.
6. Pacejka, H.B. and Besselink, I., *Tire and Vehicle Dynamics* (Butterworth-Heinemann, 2012). ISBN:9780080970165.
7. Savkoor, A.R. and Chou, C.T., "Application of Aerodynamic Actuators to Improve Vehicle Handling," *Vehicle System Dynamics* 32(4-5):345-374, 2010, doi:10.1076/vesd.32.4.345.2081.
8. https://www.grc.nasa.gov/www/k-12/airplane/geom.html.
9. Kalman, R.E., "When Is a Linear Control System Optimal?" *Journal of Basic Engineering* 86(1):51-60, 1964, doi:10.1115/1.3653115.
10. Kalman, R.E., "Contributions to the Theory of Optimal Control," *Matematica Mexicana* 5:102-119, 1960.
11. Wong, J.Y., *Theory of Ground Vehicles* (John Wiley & Sons, 2008). ISBN:9780470170380.
12. Lee, E., Kapoor, S., Sikder, T., and He, Y., "An Optimal Robust Controller for Active Trailer Differential Braking Systems of Car-Trailer Combinations," *Int. J. Vehicle Systems Modelling and Testing* 12(1-2):72-93, 2017.
13. Elbeheiry, E.M., Zeyada, Y.F., and Elaraby, M.E., "Handling Capabilities of Vehicles in Emergencies Using Coordinated AFS and ARMC Systems," *Vehicle System Dynamics* 35(3):195-215, 2001 https://doi.org/10.1076/vesd.35.3.195.2049.
14. Lee, E., "Design Optimization Active Trailer Differential Braking Systems for Car-Trailer Combinations," Master's thesis, Automotive Engineering, University of Ontario Institute of Technology, Oshawa, 2016.
15. He, Y., "Design of an Actively Controlled Aerodynamic Wing to Increase High-Speed Vehicle Safety," SAE Technical Paper 2013-01-0802, 2013, doi:10.4271/2013-01-0802.
16. Milliken, W.F. and Milliken, D.L., *Race Car Vehicle Dynamics* (SAE International, 1994).
17. Minaker, B.P. and Rieveley, R.J., "Automatic Generation of the Non-Holonomic Equations of Motion for Vehicle Stability Analysis," *Vehicle System Dynamics* 48(9):1043-1063, 2010.

Appendix 1: Notation

CG - Centre of gravity of the vehicle
δ - Steering angle of the vehicle
θ_1 - Attack angle of the right wing
θ_2 - Attack angle of the left wing
α_1 - Slip angle of left tire
α_2 - Slip angle of right tire
ψ - Yaw angle of the vehicle
y - Lateral displacement of the vehicle
V_x - Vehicle forward speed
V_y - Lateral velocity of the CG of the vehicle
Ω_z - Yaw rate of the vehicle
$\dot{V}_x$ - Longitudinal acceleration of the vehicle
$\dot{V}_y$ - Lateral acceleration of the CG of the vehicle
$\dot{\Omega}_z$ - Yaw moment of the vehicle
F_{y1} - Cornering force of the front tire
F_{y2} - Cornering force of the rear tire
F_{x1} - Longitudinal force of the front tire
F_{x2} - Longitudinal of the rear tire
F_{dr1} - Drag force of the right wing
F_{dr2} - Drag force of the left wing
F_{l1} - Lift force of the right wing
F_{l2} - Left force of the left wing
F_{z1} - Downward force on the front axle
F_{z2} - Downward force on the rear axle

ISSN 0148-7191